



Transcriptomic analysis in renal cell carcinoma and COVID-19 patients

Maha Abdulla Alwaili*

Department of Biology, College of Science, Princess Nourah bint Abdulrahman University, P.O. Box 84428, Riyadh 11671, Saudi Arabia

ARTICLE INFO

Original paper

Article history:

Received: May 24, 2023

Accepted: July 18, 2023

Published: August 31, 2023

Keywords:

COVID-19, renal cell carcinoma, differentially expressed genes, transcriptomic analysis, patients

ABSTRACT

The COVID-19 pandemic poses a heavy risk to global public health. The disease's severity and infection rate are high, especially among cancer patients. The current research was conducted to identify the most common biological pathways and how far they are associated with COVID-19 infection and clear cell renal cell carcinoma. In the current study, the authors analyzed the differentially expressed genes from the experimental and control groups with the help of the GEO2R tool. The study analyzed the protein-protein interactions that occur between the upregulated and downregulated genes from both groups based on the STRING database. In addition, the module analysis was conducted with the Cytoscape software using the MCODE plugin. The outcomes infer the upregulation of 67 genes and downregulation of 176 genes among COVID-19 patients. In the case of patients diagnosed with clear cell renal cell carcinoma, 106 genes got upregulated whereas 77 genes were downregulated. As per the outcomes achieved from the GO analysis, the differentially expressed genes play a role in C-X-C chemokine receptor activity and glycolytic process. Further, the results from the KEGG analysis establish the presence of a genetic association between HIF-1 signaling and lipid metabolism. The current study found the key genes that play a crucial role in the metabolic pathways of COVID-19 and clear cell renal cell carcinoma patients. These genes are found to be promising therapeutic targets in the prevention of complications of infection among cancer patients.

Doi: <http://dx.doi.org/10.14715/cmb/2023.69.8.24>

Copyright: © 2023 by the C.M.B. Association. All rights reserved.

Introduction

Coronavirus Disease 2019 (COVID-19) has burdened the global public health system and affected the patients' lives, their families, financial savings, and society as a whole (1-2). COVID-19 is caused by SARS-CoV2 (severe acute respiratory syndrome coronavirus 2), and the disease exhibits different symptoms in different people and goes from being asymptomatic to mild infection, fever, fatigue and severe critical illness (3-5). Some of the commonly found symptoms among COVID-19 patients include pneumonia, dry cough, dyspnea, sore throat, diarrhea, and in a few cases, the severe infection results in multi-organ failure, especially kidneys, ARDS (Acute Respiratory Distress Syndrome) which eventually results in death if left untreated (6). An individual's immune system and comorbidity status decide the disease's severity and prognosis.

The entry of the virus into the host cell remains the primary action that decides the infectivity and pathogenesis of SARS-CoV-2 (7). The binding affinity of the virus with angiotensin-converting enzyme 2 (ACE2) in humans is high (8). Renal injury remains a common symptom in severe COVID-19 patients as kidneys record high expression levels of ACE2 enzymes. SARS-CoV-2 virus induces the cytopathic effect in the podocytes of renal tissues which in turn injures the podocytes and results in proteinuria (9). COVID-19 has an increased risk of susceptibility and tends to cause the worst clinical outcomes among cancerous patients (10). In addition to the effects on cancer, COVID-19 has mitigated the survival chances of cancerous patients, especially those with renal cancer. When

cancer patients are infected with COVID-19, their lives are at stake with a higher mortality rate than the patients with the rest of the comorbidities like Diabetes Mellitus, hypertension, etc. (11).

As per the literature (12), Renal Cell Carcinoma (RCC) remains the most dangerous urologic tumor, though it makes up only 2-3% of all adult tumors. Clear cell renal cell carcinoma is one of the types of cancer diagnosed in the kidneys. When the von Hippel-Lindau gene undergoes mutation, then it upregulates the hypoxia-inducible factor which in turn enhances the proliferation rate of the cells and angiogenesis. This scenario finally results in the occurrence of clear cell renal cell carcinoma (13). Patients diagnosed with this type of cancer are highly prone to get infected with COVID-19. This is attributed to the dysfunction of the metabolic pathway among cancer patients.

In this background, the current research was conducted to identify the most commonly found biological pathways and how they correlate with COVID-19 and clear cell renal cell carcinoma. In this study, the gene array analysis was performed using the GSE53757 dataset and the GSE164805 dataset. While the former is utilized for gene expression analysis in clear cell renal cell carcinoma patients, the latter is used for gene expression analysis in SARS-CoV-2 infected patients. In the beginning, the Differentially-Expressed Genes (DEGs) were selected from both datasets. Then, protein-protein interaction was analysed. Based on the DEGs, the authors conducted the pathway analysis and KEGG to determine the biological processes.

* Corresponding author. Email: maalwaele@pnu.edu.sa

Materials and Methods

Ethics, participants, and compliance

The current retrospective study was conducted in line with the principles and standards of the Deanship of Scientific Research for Princess Nourah bint Abdulrahman University. The standards were adhered to, and the experimental procedures were conducted according to the norms. The national board of ethics officially approved the research project, namely KACST from Riyadh (KSA) with the credentials; study number H-01-R059, and IRB LOG number 20-0242. From the study participants, informed consent was obtained prior to collecting the human samples.

Collection of the dataset

Zhang Q et al. (14) created the GSE164805 dataset (<https://www.ncbi.nlm.nih.gov/geo/download/?acc=GSE164805>) which details the transcriptional profile of COVID-19 patients on the basis of their infection severity. The dataset contains five samples each from mild and severe COVID-19-infected patients whereas five healthy patient samples were collected under the control group. The sample had both males and females aged in the range of 51 to 73 years old. RNA was isolated from the peripheral blood mononuclear cells of the study patients, and RNA sequence analysis was conducted using the (HG-U133_Plus_2) Affymetrix Human Genome U133 Plus 2.0 Array.

Von Roemeling et al. (15) created the GSE53757 dataset (<https://www.ncbi.nlm.nih.gov/geo/download/?acc=GSE53757>). The dataset had data from 60 cancer patients and 40 healthy individuals. Among the study sample, 15 patients' data from each stage of the cancer were chosen for the study. After collecting the tissue samples, the gene array analysis was conducted using the Agilent-085982 Arraystar human lncRNA V5 microarray. For this study, the National Centre for Biotechnology Information Platform was used in which the Gene Expression Omnibus database was utilized for conducting the gene expression analyses (16).

Identification of DEGs in COVID-19 and RC

To find the DEGs, the GEO2R web tool (<https://www.ncbi.nlm.nih.gov/geo/geo2r/>) was utilized which compares the submitted gene dataset by leveraging the limma (linear models for microarray analysis) R package and GEO query.

The GSE164805 dataset was displayed and the classification of the samples as control and test groups was performed. After the selection was completed, the GEO2R tool was utilized to analyze the samples. In this study, the Benjamini-Hochberg method was followed to identify the statistically-significant genes expressed in the control and test groups and mitigate the False Discovery Rate (FDR) (17). The p was set at <0.05 whereas the fold change value was fixed at $|\log_2(\text{fold change})| > 1$ so as to identify the DEGs. In the case when the $\log_2FC \geq 1$, the genes are understood to be upregulated while it is said to be downregulated if the $\log_2FC \leq -1$. The inbuilt limma package, used in the tools, visualizes the DEGs present in the dataset. Once the parameters are selected, the GEO2R-based analysis is conducted which tends to tabulate the 250 DEGs. Likewise, the same procedure for DEGs was also conducted for the dataset GSE53757 and 250 significantly expressed genes were taken forward.

Protein-protein interaction analysis

To evaluate the correlation among the DEGs in COVID-19 as well as clear cell renal cell carcinoma patients, the authors conducted the protein-protein interaction (PPI) using STRING, a web-based tool (Search Tool for the Retrieval of Interacting Genes/Proteins) version 11.5 (<https://string-db.org/>) (18-20). In the STRING multiple protein sequence tab, both the upregulated as well as the downregulated genes in COVID-19 patients and the cancer patients were pasted, and PPI analysis was conducted under the bare minimum interaction confidence score set, i.e., 0.40. The analytical outcomes, i.e., protein-protein interactions are displayed, and the interaction results are analysed again using the Cytoscape software (<https://cytoscape.org/>) (version 3.9.1) (21).

The current study made use of Molecular Complex Detection (MCODE) (<http://apps.cytoscape.org/apps/mcode>) plugin to find the highly-interconnected nodes within the PPI in Cytoscape. The following parameters were used; Node Score Cut off: 0.2, Haircut: true, Fluff: false, K-Core: 2, and Maximum Depth from Seed: 100 (22), and the analysis was conducted.

Gene ontology and pathway enrichment analysis

In this study, enrichment analysis was conducted in order to determine the functions of the DEGs in COVID-19 and clear cell renal cell carcinoma patients. This gene set enrichment analysis was conducted to evaluate the gene sets that possess common biological pathways and chromosomal locations (23). Further, Gene Ontology (GO) analysis was also conducted to identify the gene products and gene annotation, which are then segregated into three elements as given herewith; 1) biological process for signal transduction or metabolic function; 2) an action's molecular function within the cell and, 3) cellular composition of the location within the cell where the gene enacts an important role (24). The Kyoto Encyclopedia of Genes and Genomes (KEGG) (25) was utilized to discover the genes' metabolic pathways. Then, Enrichr (<https://maayanlab.cloud/Enrichr/>), an online platform was utilized to analyze the GO and KEGG, and it supplied the data with regard to the genomic enrichment analysis (26). In the Enrichr platform's search box, both upregulated and downregulated genes of COVID-19 and clear cell renal cell carcinoma were fed. Then, the data was allowed to get processed so as to decode and download the biological process, molecular function, and cellular component of gene ontology and KEGG pathways.

Results

DEGs in COVID-19

Table 1 shows the details with regard to GSE164805 and GSE53757 datasets. In line with the outcomes achieved by GEO2R, we found that 67 and 176 genes were upregulated and downregulated respectively, among the COVID-19 patients. In the case of the GSE53757 dataset, the upregulation of 106 genes and the downregulation of 77 genes were found among the clear cell renal cell carcinoma patients. Table 2 shows the differentially expressed genes. The Volcano plot was used in this study to portray the DEGs in COVID-19 and cancer patients. This plot has remarkable genes with $p < 0.05$ and $\log_2FC \geq 1$ for upregulated genes and $\log_2FC \leq -1$ for downregulated genes (Figure 1).

Table 1. Details of clear cell renal cell carcinoma patients, COVID-19 patients and control groups from GSE53757 and GSE164805 datasets.

		Cancer Patients (N=60)	Healthy controls (N=40)
GSE53757	Male	NA	NA
	Female	NA	NA
	Age (years)	NA	NA
	Cancer Staging		
	Stage I	15	
	Stage II	15	
	Stage III	15	
Stage IV	15		
		COVID-19 Patients (N=10)	Healthy controls (N=5)
GSE164805	Male	9	4
	Female	1	1
	Age (years)	44-73	54-71
	Disease Severity		
	Mild infection	5	
Severe infection	5		

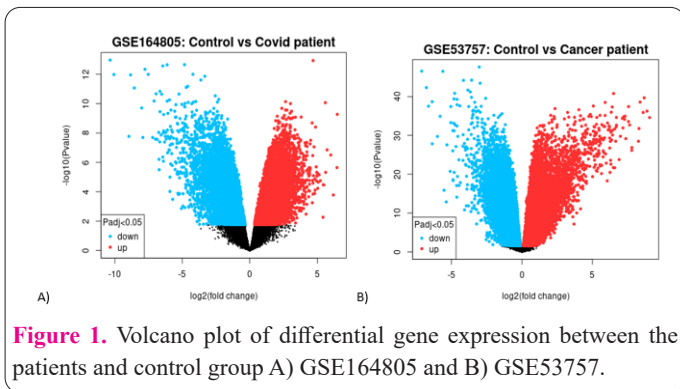


Figure 1. Volcano plot of differential gene expression between the patients and control group A) GSE164805 and B) GSE53757.

Protein-protein interaction and module analysis

As mentioned earlier the STRING platform was used to analyze the presence of functional associations among the DEGs and their protein-protein interactions. Figure 2 shows the outcomes from the STRING analysis in which there are 271 nodes and 481 edges. Here, nodes denote the number of proteins, whereas edges correspond to the type of interaction among the proteins. The PPI results were then transferred to Cytoscape so as to analyze the heavily-interconnected clusters using the MCODE. Three of the total PPI clusters were selected based on the MCODE scores, and are shown in Figure 3. Cluster 1 has a total of 14 nodes while clusters 2 and 3 have 8 and 19 nodes respectively. Table 3 shows the clusters with nodes, scores, and edges.

Gene ontology and gene set enrichment analysis

The authors analysed the gene ontology of the DEGs among COVID-19 and clear cell renal cell carcinoma patients. The outcomes infer the enrichment of the biological processes (BP) in the glycolytic process (GO:0006096), canonical glycolysis (GO:0061621), glucose catabolic process to pyruvate (GO:0061718), pyruvate metabolic process (GO:0006090) and glycolytic process through glucose-6-phosphate (GO:0061620) (Fig 4a). The DEG’s molecular function was found to have played a key role in phosphofructokinase activity (GO:0008443), ankyrin binding (GO:0030506), solute: anion antiporter activity (GO:0140323), C-X-C chemo-

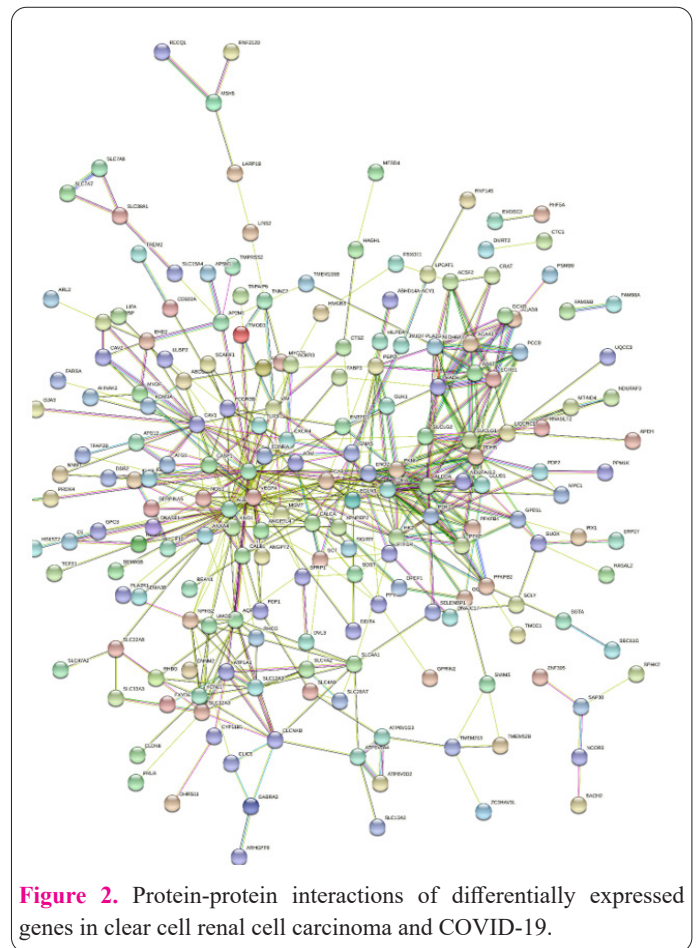


Figure 2. Protein-protein interactions of differentially expressed genes in clear cell renal cell carcinoma and COVID-19.

kine receptor activity (GO:0016494) and fructose-2,6-bisphosphate 2-phosphatase activity (GO:0004331) (Fig 4b). DEGs have the following cellular components: basolateral plasma membrane (GO:0016323), intracellular organelle lumen (GO:0070013), mitochondrial matrix (GO:0005759), endolysosome (GO:0036019) and sarcolemma (GO:0042383) (Fig 4c). These genes were identified to play a role in carbohydrate metabolism, ion transportation, and the concentration of the metal ions inside the cell. Table 4 shows the gene ontology of the DEGs.

As per the outcomes from the KEGG pathway enrichment analysis, there exists a genetic association between

Table 2. Differentially expressed genes in clear cell renal cell carcinoma and COVID-19 patients.

Differentially Expressed Genes in Clear Cell Renal Cell Carcinoma	
Upregulated genes	CALB1, KNG1, SLC22A8, UMOD, SLC12A1, TMEM213, NPHS2, SLC13A3, KCNJ1, XPNPEP2, DIO1, CLDN8, ALB, RALYL, CLCNKB, SLC4A9, SLC12A3, MUC15, FXYD4, AQP2, SERPINA5, DPEP1, ATP6V0A4, TFAP2B, DNASE1, HRG, DMRT2, SLC13A2, HS6ST2, TMEM52B, MFSD4A, Tmprss2, SFRP1, SOST, RHCG, GABRA2, RALGAPA2, LOC284578, RNF21B, SLC26A7, ATP6V1G3, PLPPR1, SLC47A2, LOC101928658, TCF21, NOS1, GGT6, FGF1, ATP6V0D2, SLC4A1, RHBG, SLC7A8, DDN, ABAT, PTH1R, ALDH6A1, CLIC5, ABHD14AACY1, ACSF2, SMIM5, IRX1, PRLR, DCXR, PLA2R1, GPC3, SUSD2, ERP27, PEPD, PFKFB2, HADH, LOC100130691, SFXN2, HYKK, SUCLG1, MAGI2AS3, GJA3, ALAD, MPC1, DANCR, ACAA1, SELENBP1, GPD1L, SAT2, ALS2CL, PCCBDHRS11, SIGIRR, C5, ECHS1, SUOX, ATP11, NAPEPLD, KCTD6, UQCRC1, PPM1K, SPHK2, AP5M1, LIN52, ACAD8, APEH, SUCLG2, PDP2, PDHB, ARL2, NDUFAF3
Downregulated genes	ANGPTL4, NDUFA4L2TNFAIP6, APOC1, LOC101928916, CD300A, LOC102724660, HK2, CA9, TREM2, HILPDA, EHD2, CDCA2, ENO2, AHNAK2, EGLN3, IGFBP3, ZNF395, BHLHE41, MIR6787, NETO2, FCGR3B, ST8SIA4, SPAG4, MIR1204, SEMA5B, ANGPT2, LPCAT1, RNASET2, FBXO16, LAMA4, MIR210HG, CAV1, CXCR4, TMCC1, PDK1, PFKP, CAV2, PFKFB4, NOL3, ADM, PLK2, ACKR3, STAMBPL1, DDB2, SAP30, TLR3, DDIT4, PAG1, CASP1, ENTPD1, ABCG1, SLC38A1, PPP1R3B, PRKCDBP, SLC15A4, PSMB8, IKBIP, VIM, VEGFA, PKM, MYOF, LIPA, FUT11, ANXA4, ZC3HAV1L, PRDX4, TMSB10, RNF149, RNF145, RECQL, SEC61G, NCOR2, LDHA, ALDOA, KDM3A
Differentially Expressed Genes in COVID-19	
Upregulated genes	AL592166.1, AC104809.2, TRIM52-AS1, DUSP9, CPA3, AP002387.1, CTSZ, LINC01198, ATG12, RAB3GAP1, HAGHL, G053003, GUK1, AL162258.1, JMJD7-PLA2G4B, MIDN, AP002748.3, MHENCR, EXOSC2, AC011442.1, BACH2, DUS1L, AC004832.3, TMEM106B, MSH5, SOCS2-AS1, MGMT, ASB18, LINC01389, G089183, HMGB3, XLOC_003734, ARHGEF9, SRD5A3-AS1, ELOA2, PARD6G, AC005906.2, LINC01619, G059429, MYOZ2, DANCR, ARMCX6, MT-ND4, AP2M1, XLOC_000223, SCT, AL392172.1, FABP3, PIK3IP1-AS1, LRRC8C-DT, CTC1, PHF5A, EDNRA, CATG00000068853.1, LINC01358, ULBP2, NDUFB2-AS1, TRIM47, MCRIP2, SGTA, NNT-AS1, ZNF529-AS1, LINC01425, LINC01588, CATG00000011211.1, LINC01605, CATG00000038197.1
Downregulated genes	TEX101, CATG00000027321.1, AC244502.1, CATG00000042513.1, ADIRF-AS1, KLK8, G023046, CATG00000066456.1, G047908, AL035696.4, TRIM6, XLOC_001908, LIPEAS1, AC105935.1, XLOC_008995, AC012594.1, G032205, AC005264.1, HAPLN2, AC006111.1, AL132819.1, CATG00000004152.1, ATG5, RSPH6A, MEIG1, XKR9, C19orf85, GLUD1, SEMA3B, CATG00000012021.1, AC022196.1, AC004233.2, G090757, AC023762.1, AC005740.3, AC007743.1, AL512444.1, CATG00000058631.1, SLC4A2, HOXC13-AS, BX255925.1, G002981, AC024587.2, AC244502.3, CATG00000117912.1, H2AFY, F10, AL138689.2, CATG00000053562.1, MARCKSL1, LINC02092, CNM2, IFT52, SLC7A7, LARP1B, BEAN1, ARHGEF1, KIAA0895L, G031345, CATG00000062999.1, RASAL2, AC126696.3, ILDR1, NKX2-2-AS1, TMEM114, IVNS1ABP, SPRN, GPRIN2, AC092723.3, AC008443.2, AC079684.1, AL513329.1, LINC01376, CALCA, CATG00000015125.1, CRAT, TPT1-AS1, KRTAP10-10, UQCC3, CATG00000098669.1, HTRA2, AC008691.1, CATG00000053260.1, FGF14-AS1, CASC18, LINC00408, LINC01191, NDUFA4L2, LCN9, C20orf24, PPP1R26AS1, FAM98B, PPY, XLOC_001935, TBC1D17, AC091948.1, AL391863.1, LINC01821, CATG00000007650.1, LINC01481, AC022148.1, AX748369, TMEM236, AL357054.3, AC106795.3, BIG-lncRNA-582, G049958, FBXO11, GNAS, XLOC_001120, AC092017.4, AC068057.1, MACROD2-AS1, CATG00000024467.1, CATG00000038258.1, DLEU2, PCDHB2, AC015849.5, FARSA, CATG00000088201.1, CYP11B1, AL161785.3, BHLHB9, XLOC_003243, DACT3-AS1, TNNC2, AC073941.1TMC3AS1, ACTB, XLOC_12_003810, USP44, AP001351.1, INTS6AS1, AC084200.1, AC010998.3, LINC00635, AL157400.3, AL049651.1, NBR2, FAM167A-AS1, TMOD3, SCARF1, DVL3, KCNN2, SAMD12, SAMMSON, CASC6, AC067930.1, G018844, ANKRD30BL, OTX1, C7orf71, ZSCAN18, AL354920.1, LOC101928303, SCLY, ARHGEF7-AS2, TALAM1, CATG00000114373.1, FCER2, SOX9-AS1, SLC35F3, AC068418.2, ZNF728, FAM98A, AC025165.3, DNAJC17, AC009145.2, LACTB2-AS1, HTN1, WFDC11, LINC02028, CATG00000079740.1, AL807776.1, AC092316.1, AC073842.1

Table 3. Highly interconnected clusters from the DEGs of GSE53757 and GSE164805 using MCODE

Cluster	Score	Nodes	Edges	Node IDs
1	6.308	14	41	ACAD8, ACSF2, ALDH6A1, CA9, ECHS1, EGLN3, GLUD1, HADH, LDHA, PCCB, PDHB, PKM, SUCLG1, ACAA1
2	5.714	8	20	HK2, PDK1, PFKFB2, PFKFB4, PFKP, VEGFA, ALDOA, ENO2
3	4.111	19	37	ANXA4, AQP2, ATP1A1, CAV1, CAV2, CLCNKB, EHD2, GNAS, KCNJ1, MYOF, NPHS2, PRKCDBP, PTH1R, RHBG, SCT, SLC12A1, VIM, ABCG1, ALB

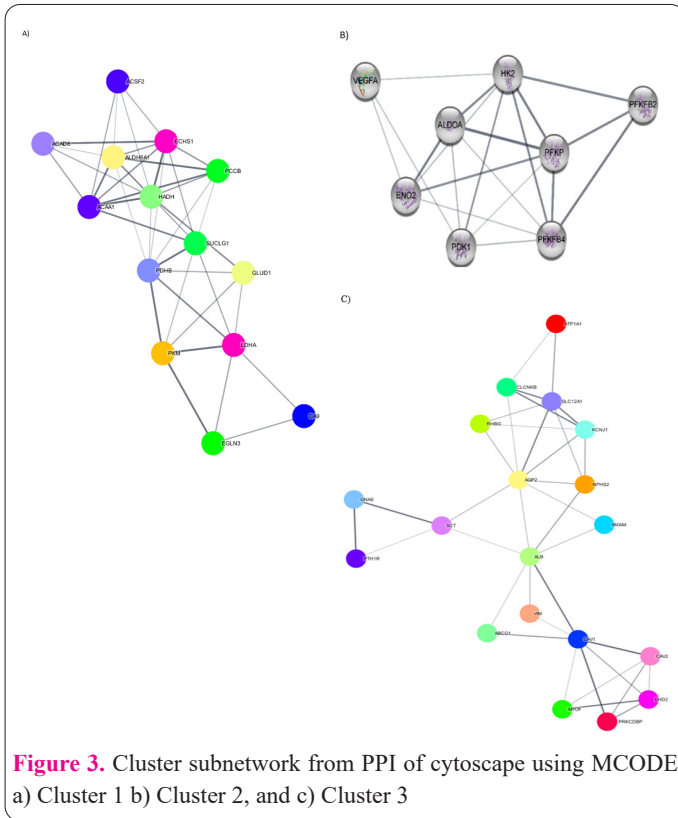


Figure 3. Cluster subnetwork from PPI of cytoscape using MCODE a) Cluster 1 b) Cluster 2, and c) Cluster 3

the DEGs in COVID-19 and cancerous patients. The mechanisms include central carbon metabolism in cancer and glycolysis/gluconeogenesis, leucine and isoleucine degradation, propanoate metabolism, valine degradation, and the HIF-1 signaling pathway. Table 5 and Figure 5 show the KEGG pathway with a list of genes.

Discussion

The current study attempts to detail the risks caused by COVID-19 infection among patients diagnosed with clear cell renal cell carcinoma. In general, it is common for cancer patients to be quickly infected as their metabolic pathways are altered, and they have low levels of immune system proteins. The current study attempted to describe the impact of SARS-CoV2 infection causing renal injury through bioinformatics. The authors conducted gene expression analysis, and the outcomes exhibit the presence of DEGs in both cancer and COVID-19-infected patients. Further, the study also established the disease prognosis

Table 5. KEGG pathway analysis of differentially expressed genes related to ccRCC and COVID-19.

Pathways	Genes
Propanoate metabolism	LDHA, ALDH6A1, ECHS1, PCCB, SUCLG2, ABAT, SUCLG1
Valine, leucine and isoleucine degradation	ACAD8, ALDH6A1, ECHS1, PCCB, ABAT, ACAA1, HADH
HIF-1 signaling pathway	LDHA, EGLN3, ANGPT2, PDHB, ENO2, ALDOA, HK2, PFKP, PDK1, VEGFA
Collecting duct acid secretion	CLCNKB, SLC4A1, ATP6V0A4, ATP6V1G3, ATP6V0D2
Glycolysis / Gluconeogenesis	LDHA, PKM, PDHB, ENO2, ALDOA, HK2, PFKP
Fructose and mannose metabolism	PFKFB2, PFKFB4, ALDOA, HK2, PFKP
Vibrio cholerae infection	SEC61G, GNAS, ATP6V0A4, ATP6V1G3, ATP6V0D2, ACTB
Central carbon metabolism in cancer	LDHA, PKM, PDHB, HK2, PFKP, PDK1
Endocrine and other factor-regulated calcium reabsorption	CALB1, GNAS, PTH1R, ATP1A1, AP2M1
Gastric acid secretion	GNAS, SLC26A7, SLC4A2, ATP1A1, KCNJ1, ACTB

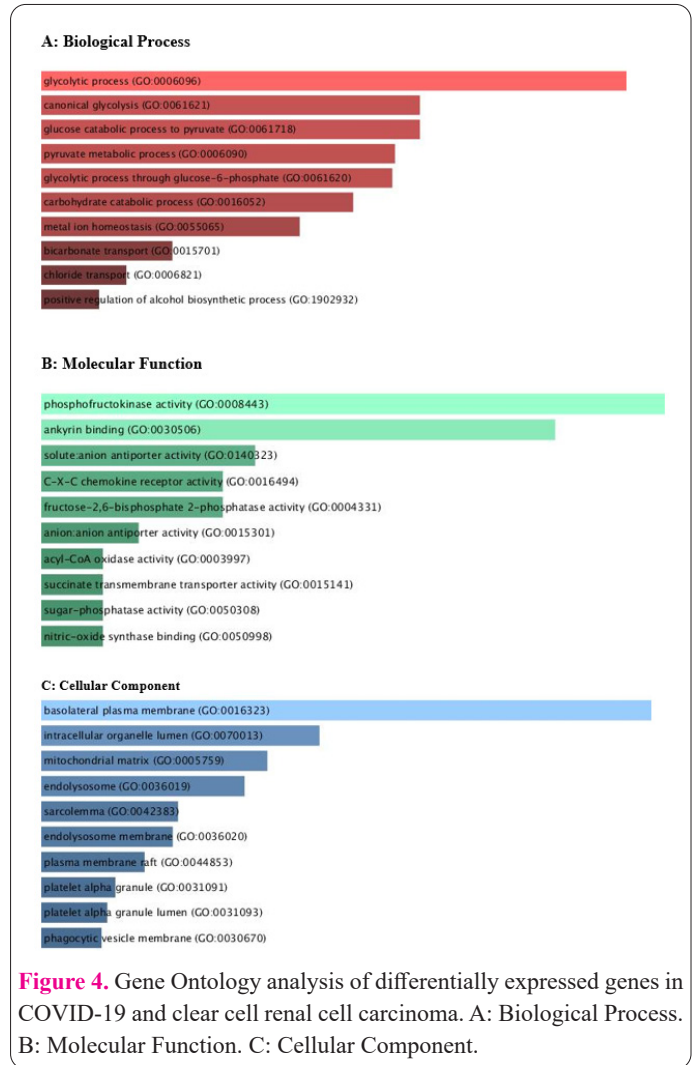


Figure 4. Gene Ontology analysis of differentially expressed genes in COVID-19 and clear cell renal cell carcinoma. A: Biological Process. B: Molecular Function. C: Cellular Component.

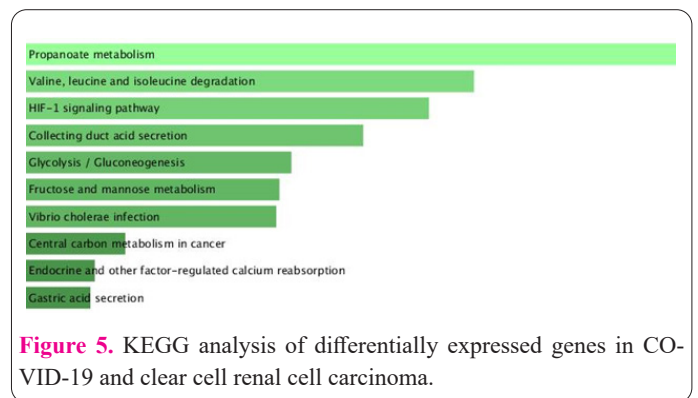


Figure 5. KEGG analysis of differentially expressed genes in COVID-19 and clear cell renal cell carcinoma.

by altering critical metabolic pathways. We found that 67 genes got upregulated, whereas 176 genes got downregulated among the COVID-19 patients. On the other hand, in clear cell renal cell carcinoma patients, 106 genes got upregulated, and 77 genes got downregulated. In addition to the above, the PPI was conducted among the DEGs, while module analysis was performed for the heavily interconnected regions. The authors performed the gene ontology and KEGG pathway analyses in addition to the network analysis.

As per the outcomes from the gene ontology analysis, the role played by DEGs in COVID-19 as well as clear cell renal cell carcinoma is crucial and is inclusive of the processes such as mitochondrial matrix and phosphofructokinase activity, glucose to pyruvate conversion, chemokine receptor signalling, glycolysis and ankyrin binding. Glucose metabolism remains a crucial element in the growth and progression of most cancers. This is attributed to the fact that glucose is the primary energy source for a cell to function while cancer cells exhibit extreme glucose metabolism or glycolysis levels. When the Warburg effect gets upregulated, it enhances the carcinogenic process and proliferation rate of the cells in clear renal cell carcinoma (27). Moreover, the glucose level in the cells decides the severity of the SARS-CoV-2 infection. According to Codo et al. (28), the glycolytic flux must happen for the viruses to replicate. The authors reported that when the key glycolytic enzymes such as 6-phospho-fructo-2-kinase/fructose 2,6 biphosphatase 3 are inhibited, it restricts the virus from replication and also prevents the initiation of cytokine responses by the dysregulated glucose metabolism. This event occurs because the said enzyme is a positive regulating factor for lactate dehydrogenase A and phosphofructokinase 1.

The pathogens that invade the body get rid of by chemokines by incorporating innate and adaptive immunocompetent cells and releasing cytotoxic factors (29). Among the COVID-19 patients, the chemokines (CXCL8, CCL2, and CXCL10 (29)) get produced and released in huge quantities due to dysregulated glucose metabolism. This, in turn, exacerbates the disease and also causes other complications. Thus, the GO analysis outcomes infer that chemokine signaling and dysregulated glucose metabolism increase the patient's mortality risk.

When the DEGs, observed in COVID-19 and clear cell renal cell carcinoma were made to undergo KEGG pathway analysis, the results infer their participation in various processes such as propanoate metabolism, valine, leucine, and isoleucine degradation, HIF-1 signal transduction, and glycolysis. Hypoxia-inducible factor 1-alpha remains a regulating factor for inflammatory response and metabolic pathways. Neoplasm, cardiovascular disease, and other infections exhibit dysregulated expression of HIF-1 α . Due to the upregulated levels of HIF-1 α in clear cell renal cell carcinoma, the patients experience the worst prognosis (30). On the other hand, the HIF-1 α triggers the replication of the virus and causes inflammation among COVID-19 patients (31). The high HIF-1 α levels observed among COVID-19 patients promote the glycolytic process and also the expression of cytokines. These processes cause oxidative stress and inflammation, resulting in a cytokine storm (32). Thus, the findings infer that the high level of HIF-1 α among cancer patients increases the risks caused by severe COVID-19 infection. The current

study has a limitation in terms of the small sample size, absence of data regarding the comorbidities, and the treatment history of the patients.

The current study established the vital role played by the dysregulated lipid and glucose metabolisms, HIF-1 signaling, and chemokine signaling among cancer patients diagnosed with COVID-19 infection. When the essential genes that play a crucial role in COVID-19-associated metabolic pathways and clear cell renal cell carcinoma patients are identified, they may act as promising therapeutic targets that prevent the complications brought by COVID-19 infection among cancer patients.

Declarations

Ethics approval and consent to participate

The retrospective study followed the principles established by the Deanship of Scientific Research for Princess Nourah bint Abdulrahman University. According to standards, all tests and research procedures have been fulfilled in accordance with norms. Therefore, the national board of ethics, namely KACST from Riyadh (KSA), has officially confirmed the research project giving the specific credentials: study number H-01-R059, IRB LOG number 20-0242.

Consent to publish

The respondents' written consent has been officially obtained before getting any human samples for research purposes.

Availability of data and materials

The gene expression data included in this study can be accessed on the GEO (Gene Expression Omnibus) database from NCBI:

GSE53757: <https://www.ncbi.nlm.nih.gov/geo/query/acc.cgi?acc=GSE53757>

GSE164805: <https://www.ncbi.nlm.nih.gov/geo/query/acc.cgi?acc=GSE164805>

Competing interests

The author declares that there is no conflict of interest.

Funding

This research was funded by Princess Nourah bint Abdulrahman University Researchers Supporting Project number (PNURSP2022R227), Princess Nourah bint Abdulrahman University, Riyadh, Saudi Arabia.

Author contributions

MAA: Conceptualization, Methodology, Software, Formal analysis, Writing - Original Draft, Review & Editing.

Acknowledgements

Princess Nourah bint Abdulrahman University Researchers Supporting Project number (PNURSP2022R227), Princess Nourah bint Abdulrahman University, Riyadh, Saudi Arabia.

References

- Zhang X, Tan Y, Ling Y, Lu G, Liu F, Yi Z, et al. Viral and host factors related to the clinical outcome of COVID-19. *Nature* 2020; 583(7816): 437-440.
- Wang T, Wu Y, Lau JYN, Yu Y, Liu L, Li J, et al. A four-compartment

- ment model for the COVID-19 infection—implications on infection kinetics, control measures, and lockdown exit strategies. *Precis Clin Med* 2020; 3(2): 104-112.
3. Chan JFW, Yuan S, Kok KH, To KKW, Chu H, Yang J, et al. A familial cluster of pneumonia associated with the 2019 novel coronavirus indicating person-to-person transmission: a study of a family cluster. *The Lancet* 2020;395(10223): 514-523.
 4. Murthy S, Gomersall CD, Fowler RA. Care for critically ill patients with COVID-19. *2020 JAMA*; 323(15): 1499-1500.
 5. Wu Z, McGoogan J M. Characteristics of and important lessons from the coronavirus disease (COVID-19) outbreak in China: summary of a report of 72 314 cases from the Chinese Center for Disease Control and Prevention. *JAMA* 2019; 323(13): 1239-1242.
 6. Sruthi U, Snehal A, Padmanabhan B. Identification of a Potent Inhibitor Targeting the Spike Protein of Pandemic Human Coronavirus, SARS-CoV-2 by Computational Methods.
 7. Shang J, Wan Y, Luo C, Ye G, Geng Q, Auerbach A, et al. Cell entry mechanisms of SARS-CoV-2. *Proc Nat Acad Sci* 2020; 117(21): 11727-11734.
 8. Xu X, Chen P, Wang J, Feng J, Zhou H, Li X, et al. Evolution of the novel coronavirus from the ongoing Wuhan outbreak and modeling of its spike protein for risk of human transmission. *Sci China Life Sci* 2020; 63(3): 457-460.
 9. Jefferson JA, Nelson PJ, Najafian B, Shankland SJ. Podocyte disorders: core curriculum 2011. *Am J Kidney Dis* 2011, 58(4), 666-677.
 10. Yang L, Chai P, Yu J, Fan X. Effects of cancer on patients with COVID-19: a systematic review and meta-analysis of 63,019 participants. *Cancer Biol Med* 2021; 18(1): 298.
 11. Mihalopoulos M, Dogra N, Mohamed N, Badani K, Kyprianou N. COVID-19 and kidney disease: molecular determinants and clinical implications in renal cancer. *Eur Urol Focus* 2020; 6(5): 1086-1096.
 12. Zequi SDC, Abreu D. Consideration in the management of renal cell carcinoma during the COVID-19 Pandemic. In *Braz J Urol* 2020; 46: 069-078.
 13. Petejova N, Martinek A. Renal cell carcinoma: Review of etiology, pathophysiology and risk factors. *Biomedical Papers of the Medical Faculty of Palacky University in Olomouc* 2016; 160(2).
 14. Zhang Q, Meng Y, Wang K, Zhang X, Chen W, Sheng J, et al. Inflammation and antiviral immune response associated with severe progression of COVID-19. *Frontiers in Immunol* 2021; 12: 631226.
 15. Von Roemeling CA, Radisky DC, Marlow LA, Cooper SJ, Grebe SK, Anastasiadis, et al. Neuronal Pentraxin 2 Supports Clear Cell Renal Cell Carcinoma by Activating the AMPA-Selective Glutamate Receptor-4NPTX2 Promotes ccRCC Malignancy. *Cancer Res* 2014; 74(17): 4796-4810.
 16. Edgar R, Domrachev M, Lash AE. Gene Expression Omnibus: NCBI gene expression and hybridization array data repository. *Nucleic Acids Research* 2002; 30(1): 207-210.
 17. Benjamini Y, Hochberg Y. Controlling the false discovery rate: a practical and powerful approach to multiple testing. *J R Stat Soc: Ser B (Methodol)* 1995;57(1): 289-300.
 18. Szklarczyk, D., Gable, A. L., Nastou, K. C., Lyon, D., Kirsch, R., Pyysalo, S., ... & von Mering, C. (2021). The STRING database in 2021: customizable protein–protein networks, and functional characterization of user-uploaded gene/measurement sets. *Nucleic Acids Res*; 49(D1): D605-D612.
 19. Szklarczyk D, Gable AL, Lyon D, Junge A, Wyder S, Huerta-Cepas J, et al. STRING v11: protein–protein association networks with increased coverage, supporting functional discovery in genome-wide experimental datasets. *Nucleic Acids Res* 2019; 47(D1): D607-D613. Szklarczyk D, Morris JH, Cook H, Kuhn M, Wyder S, Simonovic M, et al. The String database in 2017: quality-controlled protein–protein association networks, made broadly accessible. *Nucleic Acids Res* 2017 ; 45(D1):D362-D368.
 20. Shannon P, Markiel A, Ozier O, Baliga NS, Wang JT, Ramage D, et al. Cytoscape: a software environment for integrated models of biomolecular interaction networks. *Genome Res* 2013; 13(11): 2498-2504.
 21. Bader GD, Hogue CW. An automated method for finding molecular complexes in large protein interaction networks. *BMC Bioinformatics* 2003; 4(1):1-27.
 22. Subramanian A, Tamayo P, Mootha VK, Mukherjee S, Ebert BL, Gillette MA, et al. Gene set enrichment analysis: a knowledge-based approach for interpreting genome-wide expression profiles. *Proc Nat Acad Sci* 2005; 102(43):15545-15550.
 23. Doms A, Schroeder M. GoPubMed: exploring PubMed with the gene ontology. *Nucleic Acids Res* 2005; 33(suppl_2): W783-W786.
 24. Kanehisa M, Goto S. Comprehensive gene and pathway analysis of cervical cancer progression. *Nucleic Acids Res* 2000; 28: 27-30.
 25. Kuleshov MV, Jones MR, Rouillard AD, Fernandez NF, Duan Q, Wang Z, et al. Enrichr: a comprehensive gene set enrichment analysis web server 2016 update. *Nucleic Acids Res* 2016, 44(W1), W90-W97.
 26. Wang S, Zhang L, Yu Z, Chai K, Chen J. Identification of a glucose metabolism-related signature for prediction of clinical prognosis in clear cell renal cell carcinoma. *J Cancer* 2020; 11(17): 4996.
 27. Codo AC, Davanzo GG, de Brito Monteiro L, de Souza GF, Muraro SP, Virgilio-da-Silva, et al. Elevated glucose levels favor SARS-CoV-2 infection and monocyte response through a HIF-1 α /glycolysis-dependent axis. *Cell Metabol* 2020, 32(3), 437-446.
 28. Khalil BA, Elemam NM, Maghazachi AA. Chemokines and chemokine receptors during COVID-19 infection. *Comput Struct Biotechnol J* 2021;19: 976-988.
 29. Gudas LJ, Fu L, Minton DR, Mongan NP, Nanus DM. The role of HIF1 α in renal cell carcinoma tumorigenesis. *J Mol Med* 2014; 92(8): 825-836.
 30. Tian M, Liu W, Li X, Zhao P, Shereen MA, Zhu, C et al. HIF-1 α promotes SARS-CoV-2 infection and aggravates inflammatory responses to COVID-19. *Signal Transduct Target Ther* 2021; 6(1): 308.
 31. Ardestani A, Azizi Z. Targeting glucose metabolism for treatment of COVID-19. *Signal Transduct Target Ther* 2021; 6(1): 112.